CAD-Oriented Lossy Models for Radial Stubs

FRANCO GIANNINI, SENIOR MEMBER, IEEE, CLAUDIO PAOLONI, MEMBER, IEEE, AND MARINA RUGGIERI, MEMBER, IEEE

Abstract—**A lumped equivalent circuit model for both series and double-shunt (butterfly) connected radial stub has been developed. The model—simple and effective—not only includes conductor and dielectric losses but also radiation ones, which play an important role in microstrip circuit elements. Experiments widely demonstrate its suitability for implementation in available CAD programs. Furthermore, a synthesis procedure for using radial stubs in circuit design is described. An application of the above design procedure and simulation tools in the development of very broad-band nongrounded terminations is also presented.**

I. Introduction

IN MICROWAVE CIRCUITS an alternate approach for the design of biasing, filtering, matching, and virtual grounding structures by resonant straight stubs is the use of radial lines. Broad-band behavior and well-defined low impedance levels are required in both hybrid and monolithic microstrip circuits. Use of radial stubs is a solution for both of these requirements. This structure overcomes the limitation of low-impedance points, where line widths are a significant fraction of a wavelength, particularly at high frequencies. Furthermore, with respect to straight stubs, radial lines have about the same impedance level at frequencies lower or equal to the so-called resonance frequency, while maintaining the lower impedance level over a wider range [1]. Radial stubs are also space-saving and usually present a smaller outer dimension with respect to quarter-wave straight stubs at the same frequency.

Successful circuits adopting these structures have already been demonstrated [2]–[5]. Using a formula which provides the radial line input impedance [6], quite good results have been achieved at low frequencies with low-dielectric-constant substrates [7]. Characterization of radial stubs using effective dimensions and dielectric permittivities instead of actual quantities has extended to higher frequencies and substrates with higher ϵ_r techniques previously developed [8].

A complete characterization of the radial behavior is achieved with the latter method in terms of not only the conventional resonance frequency, but also the equivalent characteristic impedance presented by the radial structure. Furthermore, an accurate characterization of the inner radius has been derived, pointing out the insertion-dependent behavior of the radial stub [1], [8].

Manuscript received April 16, 1987; revised September 28, 1987.

The authors are with the Department of Electronic Engineering, Università di Roma "Tor Vergata," Rome, Italy.

IEEE Log Number 8718677.

Nevertheless, the key point for a more accurate and predictable use of radial lines in microwave circuits is the availability of a complete theoretical model which is easily adapted to available CAD programs, leading to fully automated design procedure. An equivalent lossless lumped circuit model of the radial stub has been previously developed in the case of double-shunt connection [9]. The effectiveness of this model, which is easy to implement in CAD programs, has now been extended to the case of series connection. The new model includes losses for both double-shunt and series insertion.

An extended CAD-oriented circuit is presented together with the supporting theory and an example illustrating its implementation on the Touchstone™ program. Furthermore a synthesis procedure which quickly determines the geometry of a radial stub corresponding to given requirements of a conventional straight one is described. Application of the above design procedure and simulation tools in the development of a very broad-band nongrounded termination is also shown.

II. Theoretical Characterization

The input impedance of a lossless microstrip radial stub has been previously derived by an electromagnetic (e.m.) field expansion in terms of resonant modes, assuming that only TM_{0n} modes be excited [1]. The extention of this theory to the case of lossy microstrip radial stub—in both series (Fig. 1(a)) and double-shunt connection (Fig. 1(b))—is the basis of this characterization, leading to a more accurate description of the radial line behavior.

A previous approach [10] dealt with the lossy nature of this structure, taking into account only losses due to the conductor finite conductivity and, thus, resulting in a less accurate model. In fact, the main attenuation factor is usually related to the radiation of the e.m. energy, due to the open nature of microstrip components.

The different kinds of losses can be taken into account by introducing appropriate quality factors [11] in the above-mentioned formula of the radial input impedance. Therefore, the complex impedance of a lossy radial stub can be expressed as

$$Z_{\text{in}} = \frac{1/Q_{t0} - jK_g P_{00}^2}{K^2 \epsilon_{d,0}} + j \sum_{n=1}^{\infty} \frac{K_g P_{0n}^2}{K_{0n}^2 (1 + j/Q_{t,0n}) - K^2 \epsilon_{d,n}} \quad (1)$$

0018-9480/88/0200-0305$01.00 ©1988 IEEE

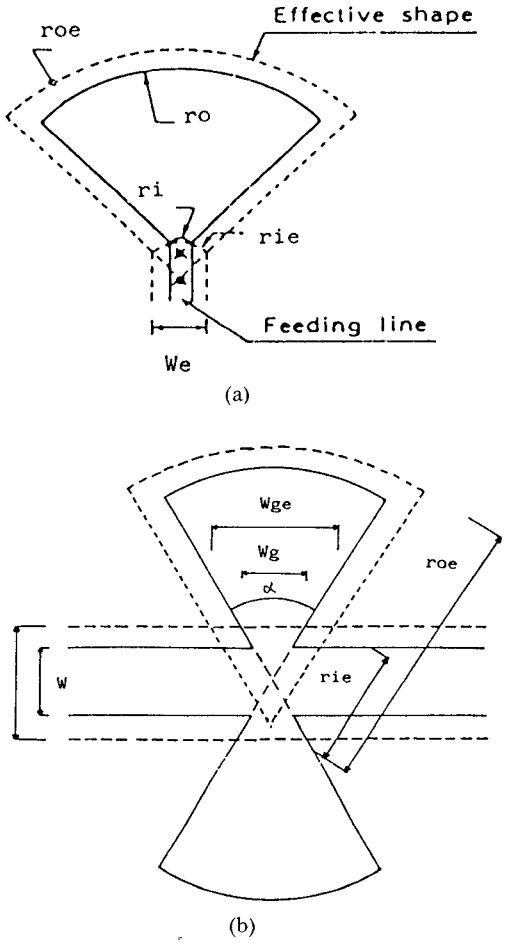

Fig. 1. (a) Series-connected radial stub. (b) Shunt-connected (butterfly) radial stub.

where

$$Q_{t0} = 1/\tan\delta$$

and

K_g	wavenumber of the feeding line,
$K = \omega\sqrt{\mu_0\epsilon_0}$	free-space wavenumber,
$\epsilon_{d,n}$	dynamic effective permettivity of the TM_{0n} mode [12],
K_{0n}	eigenvalue of the TM_{0n} mode (see Appendix),
P_{0n}	coupling coefficient between the quasi-TEM mode traveling on the feeding line and the TM_{0n} mode excited in the stub (see Appendix).

$Q_{t,0n}$ represents the global quality factor and its expression is as follows:

$$Q_{t,0n} = \left(1/Q_{d,0n} + 1/Q_{c,0n} + 1/Q_r, 0n\right)^{-1} \qquad (2)$$

where

$Q_{d,0n}$	quality factor related to losses in the dielectric,
$Q_{c,0n}$	quality factor related to losses in the conductor,
$Q_{r,0n}$	quality factor related to radiation losses.

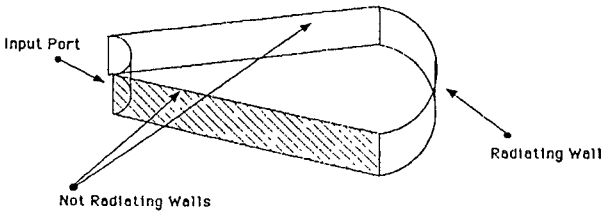

Fig. 2. Sectoral radiating structure.

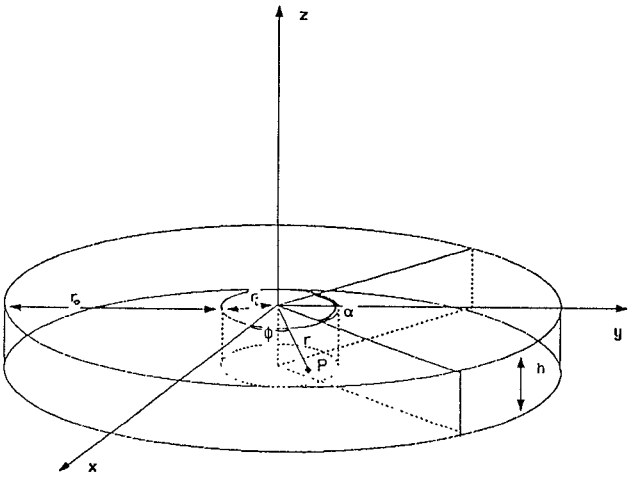

Fig. 3. Annular radiating structure.

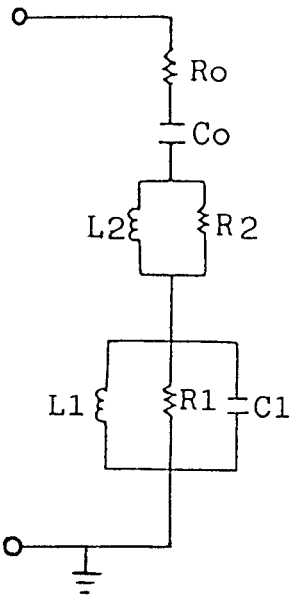

Fig. 4. Lossy lumped equivalent circuit.

The above characterization thus takes into account the three main factors of losses in the radial structure. The Q factors related to ohmic and dielectric losses are the same as those of a circular sector bounded within an angle α. They can thus be easily derived [13] for the generic TM_{0n} mode by means of the following expressions:

$$Q_{c,0n} = \left(\frac{2R_s}{\omega_{0n}\mu_0 h}\right)^{-1} \qquad (3)$$

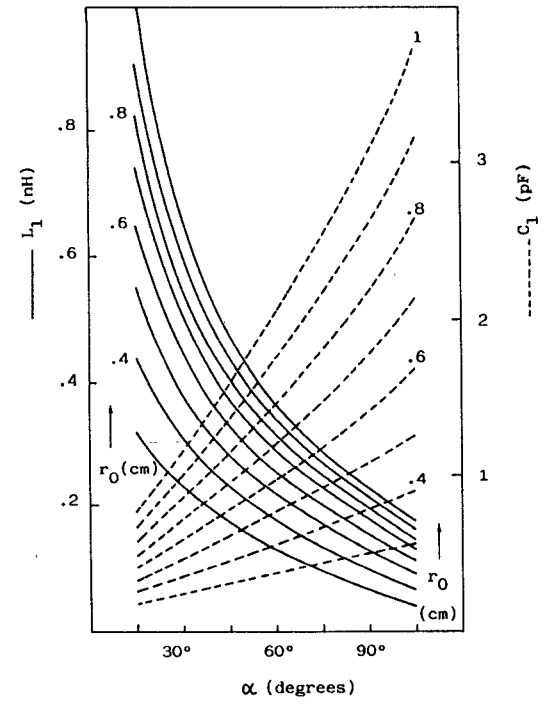

(a)

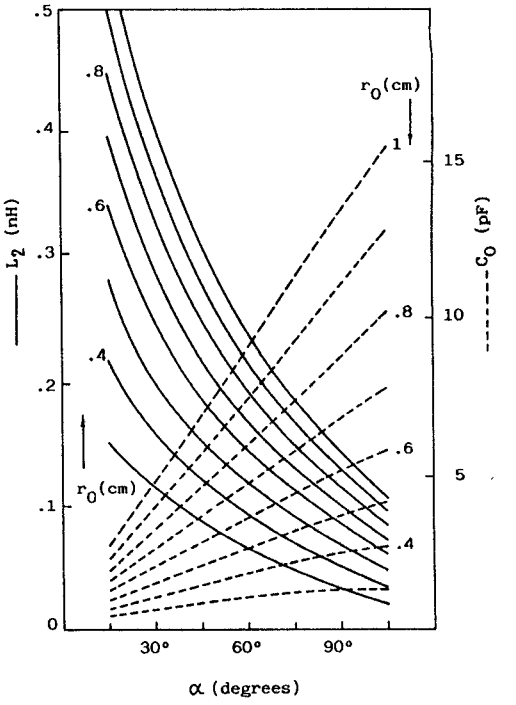

(b)

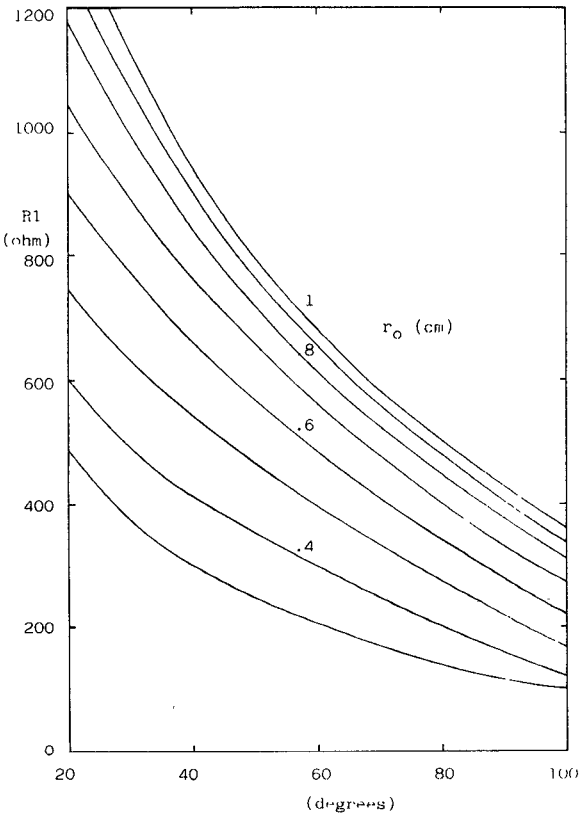

(c)

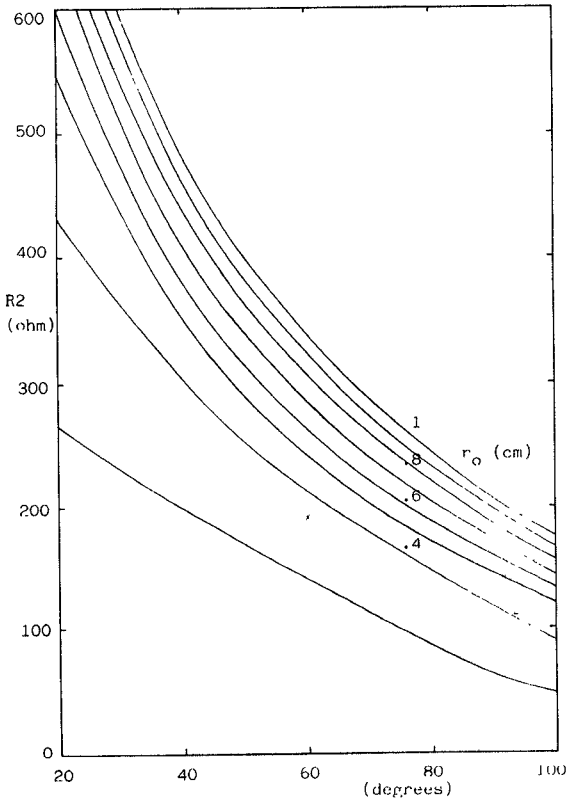

(d)

Fig. 5. Lumped equivalent circuits elements versus geometries of a single radial stub ($P = 0.3$ mm) in shunt connection (butterfly). (a) L1, C1. (b) L2, C0. (c) R1. (d) R2. Simulation has been performed on a 0.635-mm-thick substrate with $\epsilon_r = 10$.

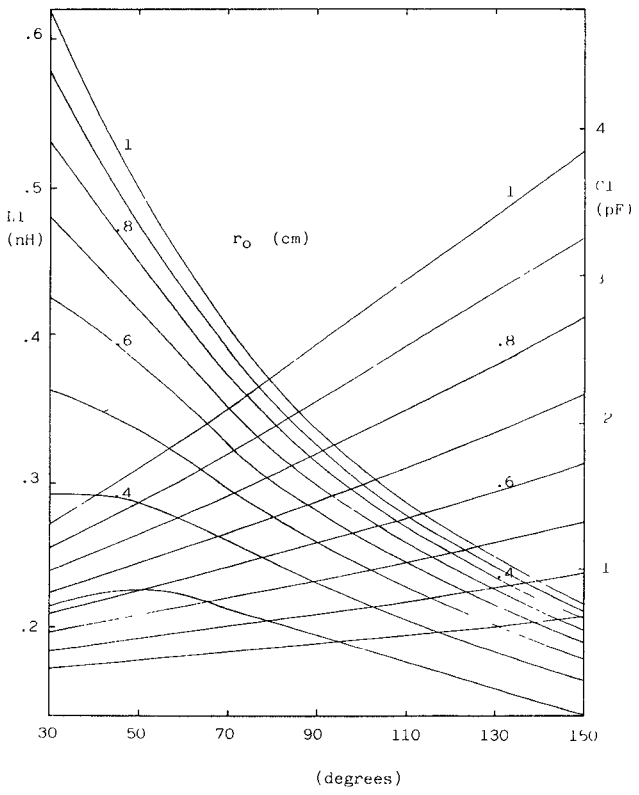

(a)

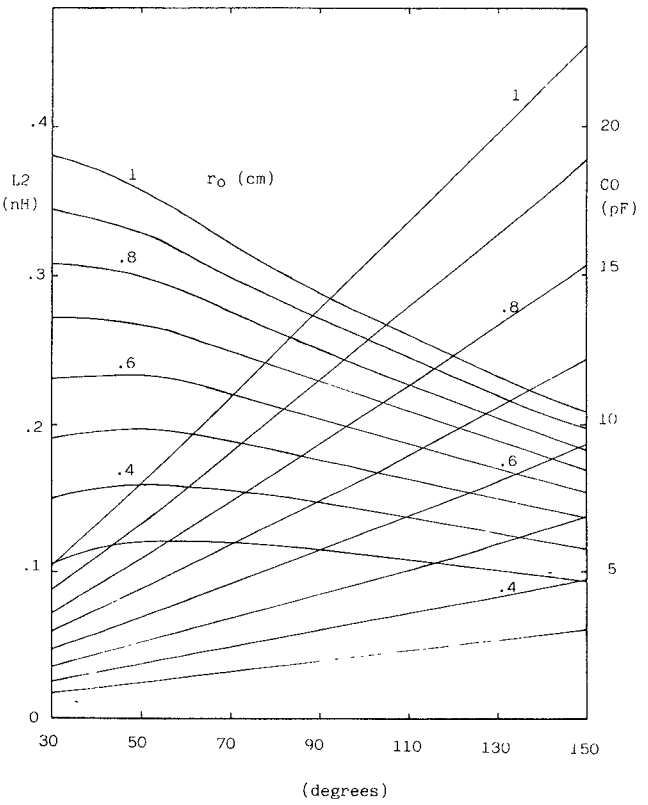

(b)

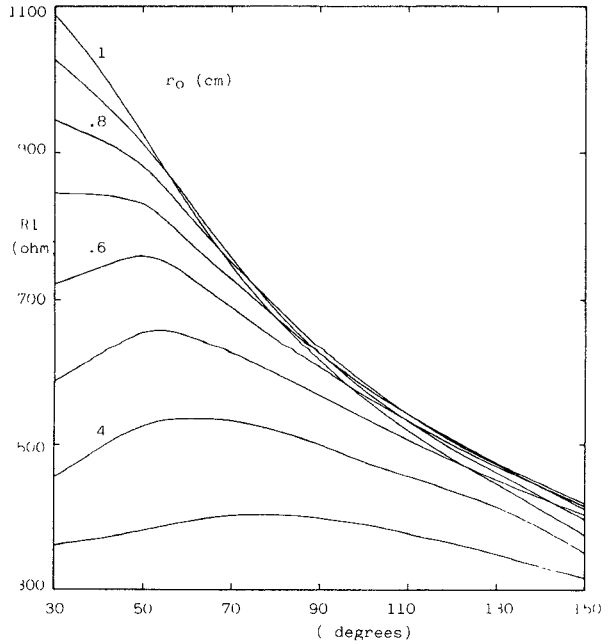

(c)

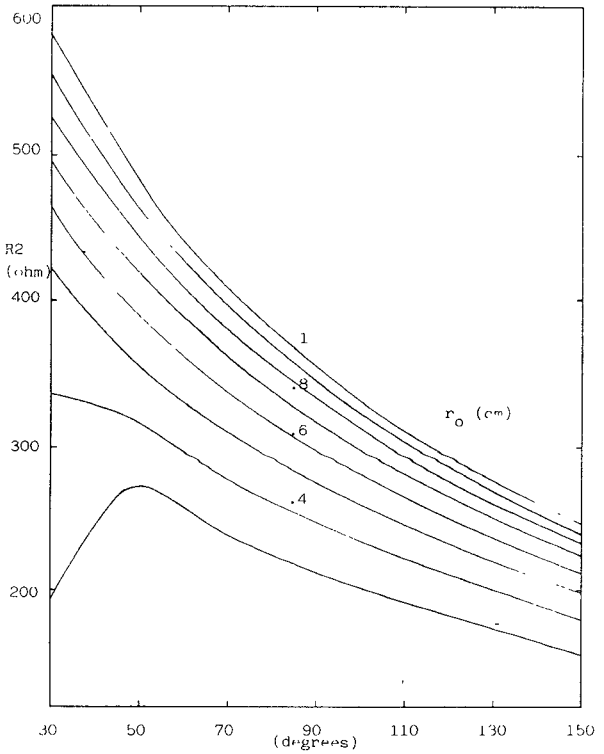

(d)

Fig. 6. Lumped equivalent circuit elements versus geometries of a series-connected radial stub (50-Ω feeding line). (a) L1, C1. (b) L2, C0. (c) R1. (d) R2. Simulation has been performed on a 0.635-mm-thick substrate with $\epsilon_r = 10$.

where R_s is the surface resistivity of the conductor, and

$$Q_{d,0n} = 1/\tan\delta \tag{4}$$

where $\tan\delta$ is the loss tangent of the dielectric substrate.

The Q factor related to radiation losses is more difficult to evaluate. A simple approach is to consider the energy related to TM_{0n} modes to be propagating in the radial direction. As a consequence, side walls can be assumed to not radiate; thus radiation losses are due only to the outer surface.

This simplifies the analysis because, for the TM_{0n} mode considered, both the power radiated from the outer surface and the stored energy inside the ring sector of angle α (Fig. 2) are equal to $\alpha/360°$ the power and energy of a ring (Fig. 3) having the same dimensions and supporting the same e.m. field on the outer radiating surface, assumed to be the only radiating one. In fact, even if the spatial e.m. field distribution sustained by the radiating sectoral aperture and the complete ring aperture is different, the starting hypothesis makes it possible to consider the total amount of power radiated by the radial stub as a fraction of the same quantity radiated by the outer surface of a ring structure. Therefore [11], the $Q_{r,0n}$ factor related to radiation losses can be expressed as follows:

$$Q_{r,0n} = \left(\frac{\omega_{0n} h \sqrt{\mu_0 \epsilon_0}}{\epsilon_{d,n}} \frac{I_\theta}{K(r_{ie}, r_{oe})} \right)^{-1} \tag{5}$$

where

$$I_\theta = \int_0^\pi J_1^2(Kr_{oe}\sin\theta)\sin\theta\, d\theta$$

$$K(r_{ie}, r_{oe}) = 1 - \frac{r_{ie}^2\{J_0(K_{0n}r_{ie})N_1(K_{0n}r_{ie}) - J_1(K_{0n}r_{ie})N_0(K_{0n}r_{ie})\}^2}{r_{oe}^2\{J_0(K_{0n}r_{oe})N_1(K_{0n}r_{ie}) - J_1(K_{0n}r_{ie})N_0(K_{0n}r_{oe})\}^2}$$

where $J_{0,1}$ and $N_{0,1}$ are the Bessel and Neumann functions of order 0 and 1, respectively.

III. The Lumped Model

The above theoretical characterization of a lossy radial stub can now be put into the form of a CAD-oriented equivalent circuit, utilizing frequency-independent lumped elements (Fig. 4). The model is valid for both double-shunt and series connection, with proper values assigned to the lumped elements.

In fact, starting with the same physical dimensions, different effective geometries for the shunt and the series connection are obtained, mainly resulting in a variation of the effective inner radius (r_{ie}). This represents a significant improvement over previously developed characterization (e.g. [7]).

The lumped model in Fig. 4 quite completely and accurately characterizes radial stub behavior. In fact it has a predictable range of validity; it adopts lumped elements; and it is substrate and insertion dependent.

The lumped elements of the equivalent circuit can be derived from the above-defined Q_{t0}, $Q_{t,01}$ and $Q_{t,0m}$ ($m > 2$), through (1)–(5), as follows:

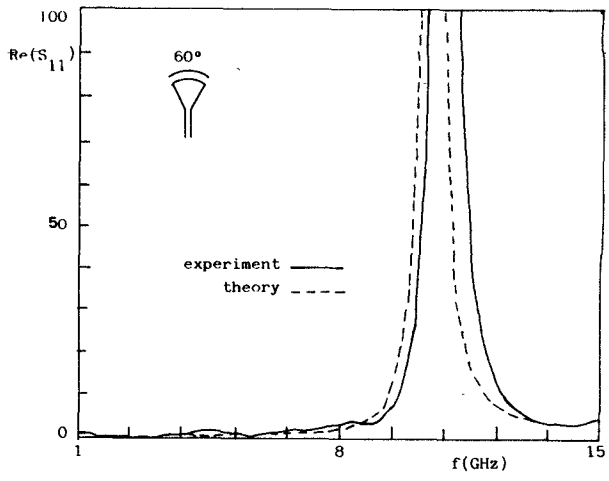

(a)

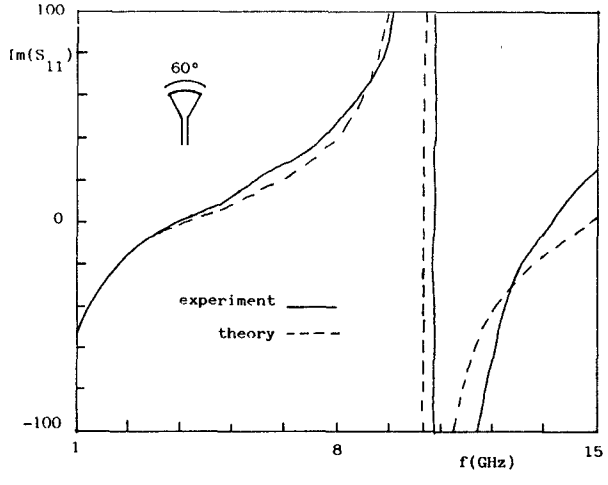

(b)

Fig. 7. Experimental and theoretical plots of input impedance for a series-connected radial stub ($r_o = 0.5$ c m, $\alpha = 60°$) realized on a 0.635-mm-thick alumina substrate ($\epsilon_r = 10$). (a) Imaginary part of input impedance. (b) Real part of input impedance.

$$R_0 = \frac{1}{Q_{t_0}\epsilon_{d,0}K^2} \qquad C_0 = \sqrt{\frac{\mu_0}{\epsilon_0\epsilon_r}}\frac{\epsilon_0\epsilon_{d,0}}{P_{00}^2} \tag{6}$$

$$R_1 = \frac{K_g P_{01}^2 Q_{t,01}}{K_{01}^2} \qquad L_1 = \frac{\sqrt{\mu_0\epsilon_0\epsilon_r}P_{01}^2}{K_{01}^2}$$

$$C_1 = \sqrt{\frac{\mu_0}{\epsilon_0\epsilon_r}}\frac{\epsilon_0\epsilon_{d,1}}{P_{01}^2}$$

$$\frac{j\omega L_2 R_2}{j\omega L_2 + R_2} = j\sum_{m=2}^{\infty}\frac{K_g P_{0m}^2}{K_{0m}^2(1 + j/Q_{tm}) - K^2\epsilon_{d,m}}.$$

The R_0 value is quite small and can be neglected, while R_1 and R_2 influence the radial stub behavior. Fig. 5(a) and (b) displays the variation of $L_i (i = 1,2)$, $C_j (j = 0,1)$ versus the radial stub geometry (angle, radii) for double-shunt connection, also known as the "butterfly" structure. The variations of R_1 and R_2 versus the same parameters are shown in Fig. 5(c) and (d). The same four plots of the

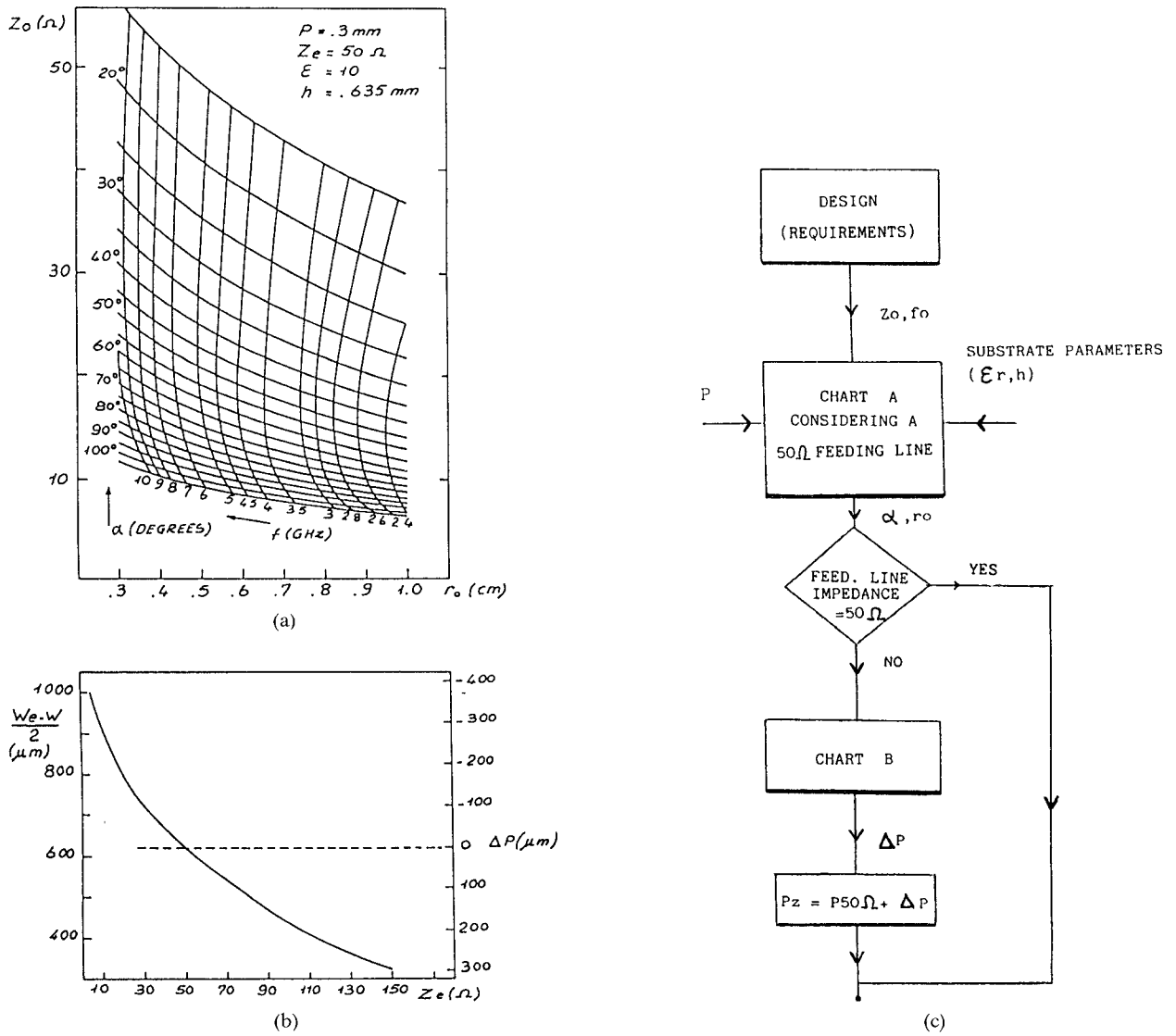

Fig. 8. (a), (b) Design charts for shunt connected radial stub. (c) Flow chart of the synthesis procedure.

series-connected radial stub are shown in Fig. 6(a), (b), (c), and (d). Starting from the physical geometries of a radial stub and going through the above plots, the corresponding lumped elements are quickly derived. Experiments on alumina ($\epsilon_r = 10$) 0.635 mm thick have fully confirmed the effectiveness of the above model. In Fig. 7 the theoretical and experimental values of the real and imaginary parts of the impedance for a series-connected radial stub are compared, displaying them in a restricted range of significant values.

Good agreement between theory and experiment is achieved at least up to a frequency (f_x) corresponding to the frequency of the first resonant mode of the radial structure ($f_x = 1/2\pi\sqrt{L_1 C_1}$), the TM_{01} in this approximation. The agreement can be extended in frequency by adding to the equivalent structure resonant cells corresponding to higher order TM_{0n} modes. Thus, a compromise between frequency effectiveness and model simplicity has to be reached. The lumped model is a complete and accurate way to represent the several dependences of the radial stub behavior. Insertion, substrate parameters, and losses can be taken into account through the lumped elements. The result is a circuit easy to implement in the available CAD programs, leading to quick and accurate analysis of the radial structure.

IV. An Application Example

In parallel to the development of lumped models to implement in CAD programs, a synthesis procedure for radial stubs has also been developed [14]. It consists of deriving the geometrical dimensions (angle α, outer radius r_o), for a fixed insertion depth (P), of a radial stub presenting the same resonance frequency (f_0) and equivalent characteristic impedance (Z_0) as a conventional straight stub. The method, here outlined for a shunt connection, utilizes two sets of curves (shown in Fig. 8(a) and (b)) where $(w_e - w)/2$ is the widening presented by the effective width of one side of the feeding line, with respect to the actual width, and Z_e represents the characteristic impedance of the feeding line. The first curve provides the

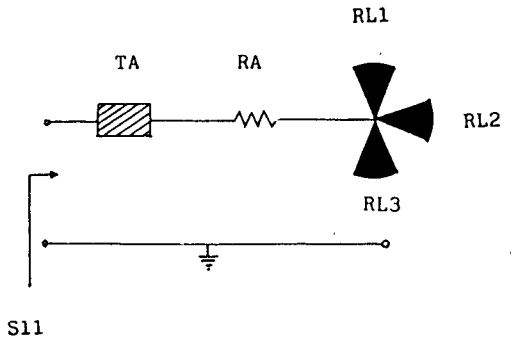

Fig. 9. Schematic of the $3\times60°$ termination.

α and r_o value corresponding to the desired f_0 and Z_0, for a given substrate and P, assuming a 50-Ω feeding line for the shunt radial stub. The second gives the actual insertion depth (P_z) to be provided with a different feeding line width.

The procedure (Fig. 8(c)), which can be fully automated, streamlines designing circuits with radial stubs. It has been successfully adopted in the development of both a two-octave stopband microstrip low-pass filter [14] and a novel termination suitable for very broad-band MIC and MMIC application [15].

The structure (Fig. 9) utilizes three radial lines and no direct grounding. The circuit has been simulated by Touchstone™ adopting the above lumped equivalent model for the radial stubs. Several samples have been developed (Duroid 6010, $\epsilon_r = 10.5$, $h = 25$ mils).

In particular, it is found that the bandwidth over which return loss is better than 20 dB, achievable with a $3\times60°$ termination, is theoretically 20 percent wider than that achieved with a 180° "half-moon" structure. This can be explained observing that—once the resonance frequency and the total angle of the termination are fixed—proper inner and outer radius values can be found in order to improve the return loss figure of the termination itself. Actually the half-moon bandwidth is further narrowed, due to the excitation of circumferential modes. In fact, these may occur if the radial stub transverse dimension is comparable to the longitudinal one, therefore when the angle is large enough (i.e., 180°) and under particular feeding conditions.

A very good agreement between theory and experiment has been obtained for the $3\times60°$ structure (Fig. 10). Also, the improvement of the above termination with respect to the theoretical and experimental performance of a conventional 180° half-moon [16] can be derived by Fig. 11. The bandwidths achieved are also wider than the ones reported for similar structures, adopting either straight [17] or single radial stub [18]. It is worth noting that $3\times60°$ configuration has to adopt different geometries to achieve the same effective ones, thus taking into account the different insertions—butterfly and series—presented by the three radial stubs of the termination. Three radial stubs with the same actual geometries, in fact, result in a configuration with a much narrower bandwidth [15]. The sensitivity of circuit response versus the resistor value has also been checked.

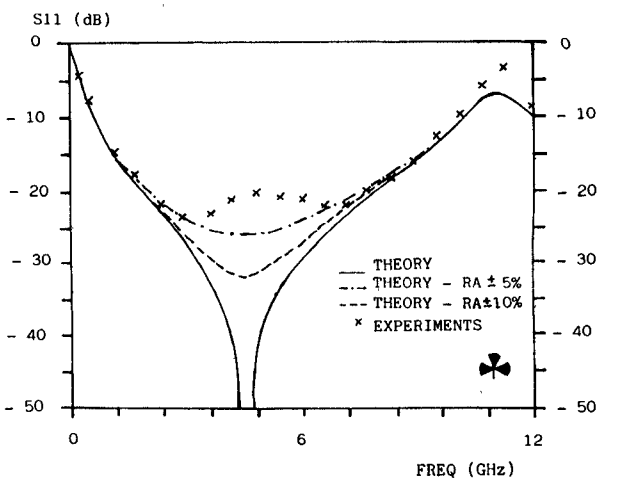

Fig. 10. Theoretical and experimental results of the $3\times60°$ termination.

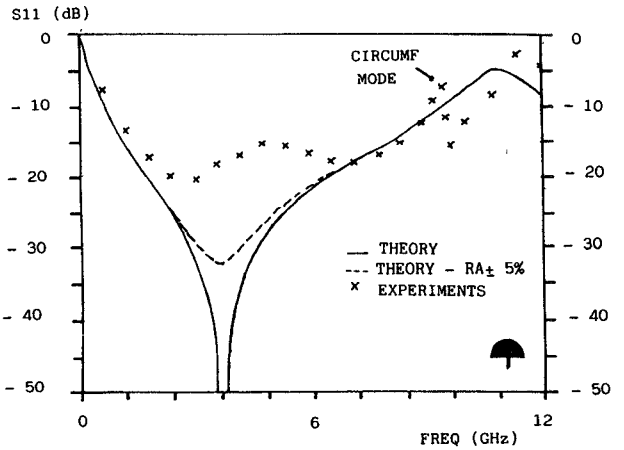

Fig. 11. Theoretical and experimental results of the 180° "half-moon" termination.

The circuits have been analyzed and optimized by Touchstone™, introducing in it the equivalent models.

V. Conclusions

The possibility of using radial stubs as broad-band and low-impedance elements has been enhanced by providing a complete set of lumped circuits modeling their electrical and insertion-dependent lossy behavior. Also, a synthesis method based upon design charts has been developed for an easy implementation of the radial stub in circuit design. The models developed have been adopted in the design of very broadband non-grounded terminations. These designs use the Touchstone™ program, in which the lossy lumped equivalent circuit for both double-shunt and series-connected radial stubs have been developed. The agreement between simulation and results is very satisfactory.

Appendix

In planar circuits, the e.m. field expansion in terms of resonant modes has already been applied to circular [19] and angular [20] structures.

First, the following eigenvalue equation has to be solved for the radial structure:

$$\nabla^2 E_{m,n} + K_{m,n}^2 E_{m,n} = 0 \tag{A1}$$

expressing the ∇ operator in circular coordinates. The solution of (A1) for the TM_{0n} modes can be written in the form

$$E_{0n} = CJ_0(K_{0n}r) + DN_0(K_{0n}r) \tag{A2}$$

where J_0, and N_0 are, respectively, the Bessel and Neumann functions of order 0. Imposing the boundary conditions at $r = r_{ie}$ and $r = r_{oe}$, K_{0n} is found as the nth root of the following equation:

$$J_0'(K_{0n}r_{oe})N_0'(K_{0n}r_{ie}) + J_0'(K_{0n}r_{ie})N_0'(K_{0n}r_{oe}) = 0. \tag{A3}$$

P_{0n}, which is the coupling coefficient between the quasi-TEM mode traveling on the feeding line and the TM_{0n} mode in the radial stub, can be expressed, according to [19], as

$$P_{0n} = \sqrt{w_{ge}}\left[A_{0n}J_0(K_{0n}r_{ie}) + B_{0n}N_0(K_{0n}r_{ie})\right]$$

$$P_{00} = \sqrt{\frac{2w_{ge}}{\alpha(r_{oe}^2 - r_{ie}^2)}} \tag{A4}$$

where

$$A_{0n} = \sqrt{\frac{2}{\alpha}}\left\{r_{oe}^2\left[J_0(K_{0n}r_{oe}) + K_nN_0(K_{0n}r_{oe})\right]^2 - r_{ie}^2\left[J_0(K_{0n}r_{ie}) + K_nN_0(K_{0n}r_{ie})\right]^2\right\}^{-1/2}$$

$$B_{0n} = K_nA_{0n} \qquad K_n = -\frac{J_1(K_{0n}r_{oe})}{N_1(K_{0n}r_{oe})}$$

where J_0, J_1, N_0, and N_1 are the Bessel and Neumann functions of order 0 and 1.

References

[1] F. Giannini, R. Sorrentino, and J. Vrba: "Planar circuit analysis of microstrip radial stub," *IEEE Trans. Microwave Theory Tech.*, vol. MTT-32, pp. 1652–1655, Dec. 1984.

[2] H. A. Atwater, "The design of the radial line stub: A useful microstrip circuit element," *Microwave J.*, pp. 149–153, Nov. 1985.

[3] A. Chu *et al.*, "Monolithic analog phase shifters and frequency multipliers from mm-wave phased array applications," *Microwave J.*, pp. 105–119, Dec. 1986.

[4] M. De Lima Coimbra, "A new kind of radial stub and some applications," in *Proc. 14th European Microwave Conf.* (Liegi), 1984, pp. 516–521.

[5] "Broadband microstrip mixer design: The Butterfly mixer." HP Application note 976.

[6] J. B. Vinding, "Radial line stubs as elements in stripline circuits," in *NEREM Records*, 1967, pp. 108–109.

[7] H. A. Atwater, "Microstrip reactive circuit elements," *IEEE Trans. Microwave Theory Tech.*, vol. MTT-31, pp. 488–491, June 1983.

[8] F. Giannini, M. Ruggieri, and J. Vrba, "Shunt-connected microstrip radial stubs," *IEEE Trans. Microwave Theory Tech.*, vol. MTT-34, pp. 363–366, Mar. 1986.

[9] F. Giannini and C. Paoloni, "Broadband lumped equivalent circuit for shunt-connected radial stub," *Electron. Lett.*, vol. 22, no. 9, pp. 485–487, Apr. 1986.

[10] S. L. March, "Analyzing lossy radial-line stubs," *IEEE Trans. Microwave Theory Tech.*, vol. MTT-33, pp. 269–271, Mar. 1985.

[11] F. Giannini, C. Paoloni, and J. Vrba; "Losses in microstrip radial stubs," in *Proc. 16th European Microwave Conf.* (Dublin), 1986, pp. 523–528.

[12] J. Vrba, "Dynamic permittivities of microstrip ring resonators," *Electron. Lett.*, vol. 15, no. 16, pp. 504–505, Aug. 1979.

[13] I. J. Bahl and P. Barthia, *Microstrip Antennas*. Dedham, MA: Artech House, 1982.

[14] F. Giannini, M. Salerno, and R. Sorrentino: "Two-octave stopband microstrip low-pass filter design," in *Proc. 16th European Microwave Conf.* (Dublin), 1986, pp. 292–297.

[15] F. Giannini and M. Ruggieri, "A broadband termination utilizing multiple radial line structure," in *Proc. MIOP*, vol. 2, no. 6B1, (Wiesbaden, Germany), May 1987.

[16] B. A. Syrett, "A Broadband element for microstrip bias or tuning circuits," *IEEE Trans. Microwave Theory Tech.*, vol. MTT-28, pp. 925–927, Aug. 1980.

[17] I. J. P. Linner and H. B. Lunden, "Theory and design of broadband nongrounded matched loads for planar circuits," *IEEE Trans. Microwave Theory Tech.*, vol. MTT-34, pp. 892–896, Aug. 1986.

[18] A. M. Khilla, "Accurate closed-form expressions for ring and disc-type microstrip resonators," *Microwave J.*, vol. 27 no. 11, pp. 91–105, 1984.

[19] G. D'Inzeo, F. Giannini, C. M. Sodi, and R. Sorrentino, "Method of analysis and filtering properties of microwave planar networks," *IEEE Trans. Microwave Theory Tech.*, vol. MTT-26, pp. 462–471, July 1978.

[20] G. D'Inzeo, F. Giannini, R. Sorrentino, and J. Vrba, "Microwave planar networks: The annular structure," *Electron. Lett.* vol. 14, no. 16, pp. 526–528, Aug. 1978.

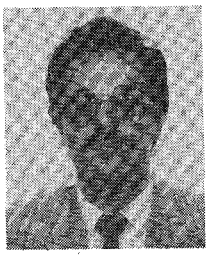

Franco Giannini (M'82–SM'84) was born in Galatina, Italy, on November 9, 1944. He received the degree in electronics engineering from the University of Rome "La Sapienza" in 1968.

In 1968 he joined the Institute of Electronics of "La Sapienza," where he was Assistant Professor until 1980. He was also Associate Professor of Microwaves at the University of Ancona, Italy (1973–1974), and of both Solid-State Electronics (1974–1977) and Applied Electronics (1977–1980) at the University of Rome "La Sapienza." In 1980 he became Full Professor of Applied Electronics at "La Sapienza."

Since 1981 he has been with the II University of Rome "Tor Vergata." He has been working on problems concerning theory of active and passive microwave components, including GaAs monolithic circuits. He is presently chairing the theme "Monolithic Integrated Circuits in the 20–30 GHz bandwidth" of the CNR's National Project "Solid State Electronic Devices." He is author and coauthor of more than 80 technical papers.

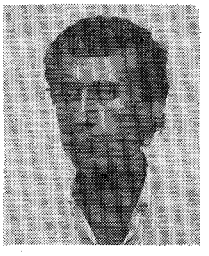

Claudio Paoloni (S'84–M'84) was born in Rome, Italy, on August 11, 1959. He received the degree in Electronics engineering from the University of Rome "La Sapienza" in 1984. His thesis was on design and realization of a microwave low-noise amplifier supported by Elettronica S.p.A.

In 1984 he took a fellowship at FACE (ITT) Research Center (Pomezia, Italy), where he designed and developed a low-noise amplifier for DBS. He was also a consultant at the Fondazione "Ugo Bordoni" on mm-wave oscillators and

at MICREL s.r.l. in the field of high-performance low-noise amplifiers. He is presently a Research and Teaching Assistant in the Department of Electronics Engineering of the II University of Rome "Tor Vergata." His research mainly concentrates on microwave planar circuit characterization of active circuit design (amplifiers, oscillators).

✠

Marina Ruggieri (S'84–M'85) was born in Napoli, Italy, on April 29, 1961. She received the degree in Electronics Engineering in 1984 from the University of Rome "La Sapienza." Her thesis was on the development of a DGFET mixer for the 12-GHz DBS receiver and it was performed during a fellowship period at the FACE (ITT) Research Center, Pomezia, Italy.

She was with FACE (ITT) (1985–1986) in the High Frequency Division. During that period she studied the feasibility of the DBS receiver in GaAs monolithic technology and was sent to the Gallium Arsenide Technology Center (GTC-ITT, Roanoke, VA) for training on GaAs MMIC design (low-noise and feedback amplifiers, mixers, oscillators, phase shifters) and fabrication techniques. After returning to Rome, she mainly worked on the development of a flat antenna and the design of mm-wave circuits. She is presently a Research and Teaching Assistant in the Department of Electronics Engineering of the II University of Rome "Tor Vergata." Her research mainly concerns microwave/communication circuit characterization and design.